Optics & Laser Technology 54 (2013) 428–431

Contents lists available at SciVerse ScienceDirect

Optics & Laser Technology

journal homepage: www.elsevier.com/locate/optlastec

Sub-micron structuring of silicon using femtosecond laser interferometry

V. Oliveira [a,c,*], R. Vilar [b,c], R. Serra [d], J.C. Oliveira [d], N.I. Polushkin [b,c], O. Conde [c,e]

[a] Instituto Superior de Engenharia de Lisboa, Avenida Conselheiro Emídio Navarro no 1, 1959-007 Lisboa, Portugal
[b] Instituto Superior Técnico, Avenida Rovisco Pais no 1, 1049-001 Lisboa, Portugal
[c] ICEMS - Instituto de Ciência e Engenharia de Materiais e Superfícies, Avenida Rovisco Pais no 1, 1049-001 Lisboa, Portugal
[d] CEMUC - Centro de Engenharia Mecânica da Universidade de Coimbra, Departamento de Engenharia Mecânica, Universidade de Coimbra, Rua Luís Reis Santos, 3030-788 Coimbra, Portugal
[e] Faculdade de Ciências da Universidade de Lisboa, Departamento de Física, Campo Grande Ed. C8, 1749-016 Lisboa, Portugal

ARTICLE INFO

Article history:
Received 16 May 2013
Received in revised form
27 June 2013
Accepted 28 June 2013
Available online 24 July 2013

Keywords:
Silicon patterning
Femtosecond laser
Michelson interferometer

ABSTRACT

We report the fabrication of planar sub-micron gratings in silicon with a period of 720 nm using a modified Michelson interferometer and femtosecond laser radiation. The gratings consist of alternated stripes of laser ablated and unmodified material. Ablated stripes are bordered by parallel ridges which protrude above the unmodified material. In the regions where ridges are formed, the laser radiation intensity is not sufficient to cause ablation. Nevertheless, melting and a significant temperature increase are expected, and ridges may be formed due to expansion of silicon during resolidification or silicon oxidation. These conclusions are consistent with the evolution of the stripes morphology as a function of the distance from the center of the grating.

1. Introduction

Surface patterning using pulsed lasers and holographic optical set-ups proved to be a powerful and versatile tool for micro-machining and patterning [1–6]. The principle of holographic surface patterning is simple: when two or more pulses of coherent radiation overlap in time and space, an interference pattern is generated that can be used to imprint periodic structures on a material surface. Femtosecond lasers are particularly attractive for this purpose, as compared to continuous-wave and long-pulse duration lasers [7,8] because, due to their extremely short pulse duration, a very high peak power is achieved. As a result, non-linear effects and a plasma-mediated ablation mechanism that minimizes collateral thermal effects are favored [7–9]. Taking advantage of this, high quality periodic micro and nanostructures were successfully fabricated using femtosecond laser radiation and interferometric techniques in bulk transparent dielectric materials [4,10], metals [5,11] and thin films [3,12]. Due to the importance of silicon in the microelectronic and solar cell industries, Si surface texturing using femtosecond laser radiation has been extensively reported in the literature. The large majority of the studies on Si texturing deal with the formation of self-organized arrays of microcones [13,14] or sub-wavelength laser-induced periodic surface structures [15,16] created by irradiating silicon with multiple femtosecond laser pulses of near-IR radiation, and aimed at controlling the material wettability [17,18], optical properties [19], or field emission efficiency [20]. In contrast, only a few studies report the formation of periodic patterns in silicon using femtosecond laser interferometry [21,22]. Tan et al. [21] successfully fabricated planar gratings with periods between 1.6 and 4.0 μm in bulk silicon, using a Mach–Zender interferometer and radiation from a Ti-Sapphire laser (400 nm wavelength, 200 fs pulse duration). The main drawback of this Mach–Zender interferometer is the minimum achievable gratings period which depends on the ratio D/f, where D is the focusing lens diameter and f its focal length. As a result, in order to achieve sub-micron structures with common near-infrared lasers ($\lambda \sim 1$ μm), lenses with a D/f ratio greater than 1 must be used. In this paper, we describe the fabrication of sub-micron planar gratings on silicon using a modified Michelson interferometer and a single femtosecond laser pulse. The main advantages of this setup with respect to those reported previously are the simplicity of the interferometer design and alignment, the possibility of sub-micron structuring using ordinary focusing lenses, and of the procedure used to monitor time coincidence. The work presented shows that femtosecond laser interferometry may be used to create versatile nanoscaled structures such as silicon nanowires for sensing applications [23].

2. Materials and methods

All experiments were performed in air on 500 μm thick Si (100) wafers. Processing was carried out with a commercial Yb:KYW

* Correspondence to: Instituto Superior de Engenharia de Lisboa, Avenida Rovisco Pais no 1, 1049-001 Lisboa, Portugal. Tel.: +351 218 317 135; fax: +351218317138.
E-mail address: voliveira@adf.isel.pt (V. Oliveira).

0030-3992/$ - see front matter © 2013 Elsevier Ltd. All rights reserved.
http://dx.doi.org/10.1016/j.optlastec.2013.06.031

chirped-pulse-regenerative amplification laser system (Amplitude Systèmes, s-Pulse HP) providing linearly polarized laser pulses with 560 fs duration at a central wavelength $\lambda = 1030$ nm. The patterns were produced using a beam delivery system based on a Michelson interferometer, similar to the one previously used to create sub-micron patterns in thin-film magnetic alloys [24] (Fig. 1(a)). In this optical set-up, the laser beam is firstly split in two by a non-polarizing beam splitter. Beams 1 and 2 are reflected by mirrors M1a and M2a, respectively and, after crossing the beam splitter, directed to the focusing lenses FL1 and FL2 by mirrors M1b and M2b, respectively. Finally, the two beams are directed to the same area on the sample's surface by mirrors M1c and M2c. The fringe spacing is given by $d = \lambda/[2\sin(\theta/2)]$, where λ denotes the radiation wavelength and θ the angle between the interfering beams. The angle θ depends on the distance between the mirrors M1c and M2c, D, and between the sample and the line defined by the centers of the two mirrors, L. It results from simple trigonometry that $\theta/2 = \tan^{-1}(D/2L)$. The fringes spacing can be controlled by changing either D or L. In the present study, $D = 40$ mm and $L = 18$ mm, leading to a fringe spacing $d \sim 700$ nm. In order to overlap the two beams in time, the optical path length of beam 2 can be controlled by a precise translation of mirror M2a. To detect time coincidence, the sample is substituted by a common 3M post-it green paper, and the paper two-photon fluorescence monitored by a video camera. Because the two-photon absorption is proportional to the square of the light intensity, the light intensity emitted by the paper increases when time coincidence occurs. This is demonstrated in Fig. 1(b) where images of the light emitted by the paper before and after time coincidence are depicted. After processing, the surfaces were observed by scanning electron microscopy (SEM) and atomic force microscopy (AFM). SEM was performed using a JEOL 7001 field-emission scanning electron microscope (FE-SEM). AFM measurements were carried out in air and at room temperature with a Brunker Innova system in tapping mode using a Si probe with 8 nm tip radius.

3. Results and discussion

The conditions for gratings production were optimized by varying the laser pulse energy. Good quality and approximately circular gratings with about 125 μm diameter were produced by the interference of two 100 μJ laser pulses. The gratings consist of parallel stripes with a constant period of about 720 nm, in good agreement with the predicted 700 nm. Figs. 2 and 3 depict SEM and AFM images of the central region of a grating. The dark stripes in the SEM image correspond to higher radiation intensity regions, where silicon was ablated, while the bright stripes correspond to regions of lower radiation intensity, where no significant modifications occurred. Interestingly, the ablated stripes present 80 nm wide longitudinal parallel ridges at each side, separated by ~340 nm. The AFM topographic profile of Fig. 3(b) shows that these ridges typically protrude 3–4 nm above the original surface level, and the ablated regions are 1–2 nm deep.

We calculated the radiation intensity distribution at the target surface, I. Assuming that the spatial radiation intensity distribution of the two interfering beams is the same, I can be expressed as

$$I = 2I_0[1 + \cos(2\pi x/d)], \quad (1)$$

where d is the fringe period and I_0 the interfering beams intensity distribution. Assuming that the interfering beams are Gaussian

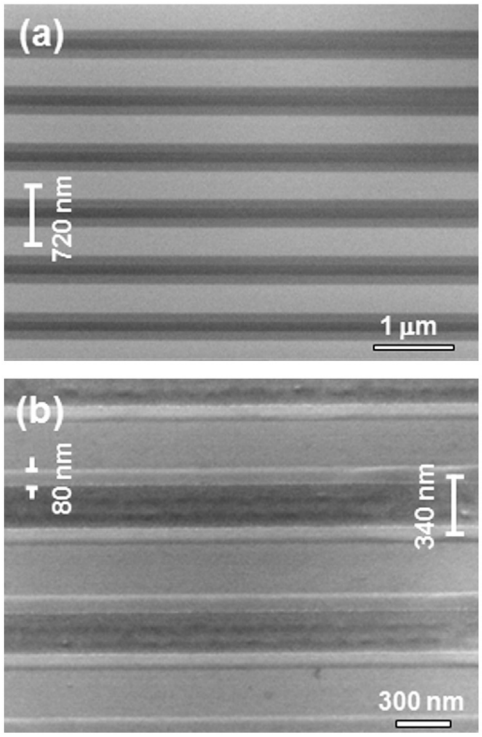

Fig. 2. (a) Top view FE-SEM image of the central region of a grating created in silicon using single laser pulse; (b) its magnified view tilted by 30°.

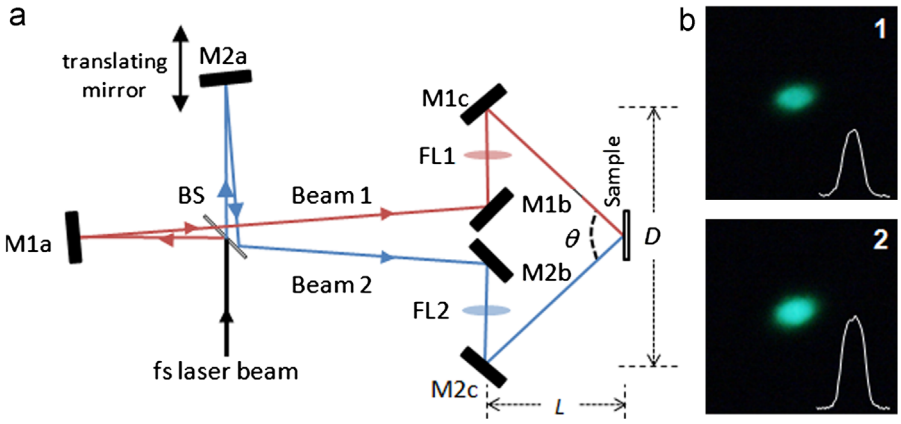

Fig. 1. (a) Optical scheme for direct laser interference patterning. The notations used are as follows: BS is beam splitter, M1a ((b) and (c)) and M2a ((b) and (c)) are mirrors for beam 1 and 2, FL 1(2) are focusing lenses. Mirror M2a was mounted on a translation stage for finding overlapping in time by adjusting a time delay between the beams. (b) Images and intensity profile (inset) of the light emitted by a common green paper when (1) the interfering beams are not coincident in time; and (2) the interfering beams are coincident in time.

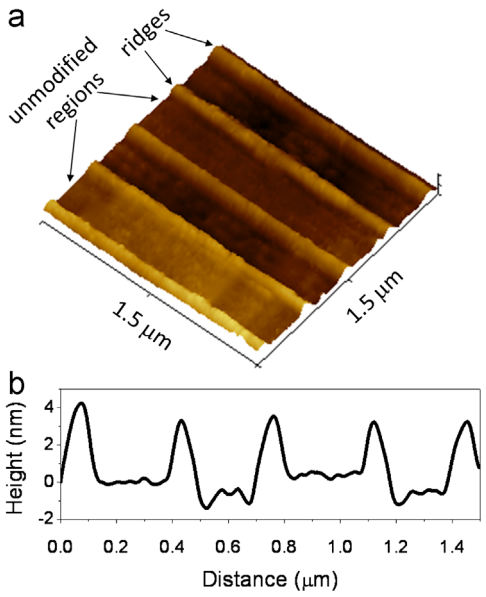

Fig. 3. (a) AFM image of the central region of a grating and (b) the corresponding cross-sectional topographic profile.

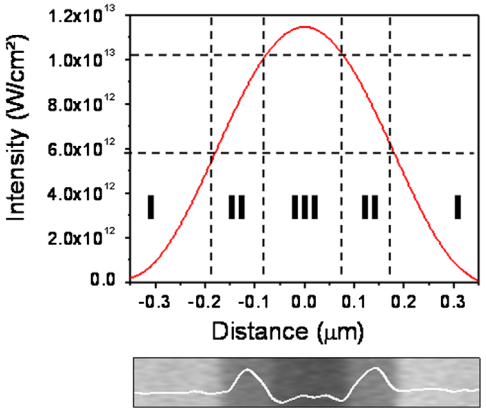

Fig. 4. Calculated radiation intensity profile in the vicinity of a stripe in the center of the grating and corresponding FE-SEM image and AFM topographic profile.

and square laser pulses, I_0 is given by

$$I_0 = \frac{2E}{\tau\pi w^2} e^{-2r^2/w^2} \quad (2)$$

where E is the pulse energy, τ is the pulse duration, r is the radial distance, and w is the grating radius. The radiation intensity distribution calculated using Eq. (1), taking $E=100$ μJ, $w=62.5$ μm, $\tau=560$ fs and $r=0$ is depicted in Fig. 4 together with the FE-SEM image of a stripe obtained in the central region of the grating using these parameters. The ablated region III corresponds to radiation intensities in the range of $1.0–1.2\times10^{13}$ W/cm^2. The protruding ridges (region II) correspond to radiation intensities in the range of $0.6–1.0\times10^{13}$ W/cm^2. Finally, the unmodified material (region I) correspond to radiation intensities below 0.6×10^{13} W/cm^2. Based on the above considerations, the grating profile is explained as follows. In region III, silicon is ablated because the radiation intensity is higher than the ablation threshold. On the contrary, in region II the radiation intensity is below the ablation threshold and ablation do not occur. Nevertheless, melting and a significant temperature increase are expected. As a result, the protruding ridges may be formed due to melting followed by expansion of silicon during resolidification [25,26], or, since the laser treatment was performed in air, due to silicon oxidation favored by the temperature increase in these regions [27,28]. Finally, in region I, the radiation intensity is insufficient to cause significant visible changes in the target material.

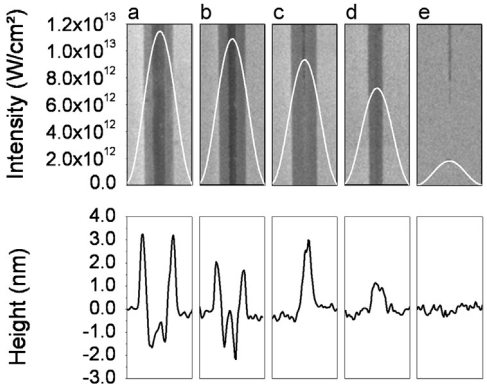

Fig. 5. SEM images and AFM profiles of the same stripe as a function of the distance r from the grating center, and corresponding intensity profile calculated using Eq. (1): (a) $r=0$; (b) $r=10$ μm; (c) $r=20$ μm; (d) $r=30$ μm; and (e) $r=60$ μm.

The proposed explanation is consistent with the evolution of the pattern profile from the center of the grating to its periphery. Fig. 5 shows FE-SEM images and AFM topographic profiles of the same stripe at different distances from the grating center, and the corresponding radiation intensity distribution calculated using Eq. (1). In the central region of the gratings where the radiation intensity is maximum, the three distinct regions previously mentioned are observed (Fig. 5a and b), but in the periphery of the grating only two regions are observed because the radiation intensity was not sufficient to cause ablation (Fig. 5c and d). Finally, at the border of the grating, the radiation intensity is too small to cause any significant changes in the material.

4. Conclusions

In summary, planar gratings with a period of about 720 nm nanometers were produced in silicon by single-pulse laser treatment using a modified Michelson interferometer and femtosecond laser radiation. The gratings consist of alternated stripes of ablated and unaffected material. The ablated stripes are surrounded by parallel ridges separated of about 340 nm which protrude 3–4 nm above the initial surface. The laser radiation intensity in the regions of ablated stripes is high enough to cause ablation. On the contrary, in the regions where ridges are formed melting and a significant temperature increase is expected. As a consequence, ridges may be formed due to silicon expansion during resolidification or oxidation.

Acknowledgments

Work was supported by the Portuguese Foundation for Science and Technology (FCT) through the Project PTDC/FIS/121588/2010 and Grant SSFRH/BPD 17382712010 (R.S.).

References

[1] Rezek B, Nebel CE, Stutzmann M. Interference laser crystallization of microcrystalline silicon using asymmetric beam intensities. Journal of Non-Crystalline Solids 2000;266:650–3.
[2] Kaganovskii Y, Vladomirsky H, Rosenbluh M. Periodic lines and holes produced in thin Au films by pulsed laser irradiation. Journal of Applied Physics 2006;100:044317.
[3] Kawamura K, Sarukura N, Hirano M, Hosono H. Holographic encoding of fine-pitched micrograting structures in amorphous SiO_2 thin films on silicon by a single femtosecond laser pulse. Applied Physics Letters 2001;78:1038–40.

[4] Kawamura K, Sarukura N, Hirano M, Ito N, Hosono H. Periodic nanostructure array in crossed holographic gratings on silica glass by two interfered infrared-femtosecond laser pulses. Applied Physics Letters 2001;79:1228–30.
[5] Oliveira V, Polushkin NI, Conde O, Vilar R. Laser surface patterning using a Michelson interferometer and femtosecond laser radiation. Optics and Laser Technology 2012;44:2072–5.
[6] Venkatakrishnan K, Sivakumar NR, Tan B. Fabrication of planar gratings by direct ablation using an ultrashort pulse laser in a common optical path configuration. Applied Physics A: Materials Science and Processing 2003;76:143–6.
[7] Chichkov BN, Momma C, Nolte S, von Alvensleben F, Tunnermann A. Femtosecond, picosecond and nanosecond laser ablation of solids. Applied Physics A: Materials Science and Processing 1996;63:109–15.
[8] Liu X, Du D, Mourou G. Laser ablation and micromachining with ultrashort laser pulses. Journal of Quantum Electronics 1997;33:1706–16.
[9] Gamaly EG, Rode AV, Luther-Davies B, Tikhonchuk VT. Ablation of solids by femtosecond lasers: ablation mechanism and ablation thresholds for metals and dielectrics. Physics of Plasmas 2002;9:949–57.
[10] Hirano M, Kawamura K, Hosono H. Encoding of holographic grating and periodic nano-structure by femtosecond laser pulse. Applied Surface Science 2002;197–198:688–98.
[11] Venkatakrishanan K, Sivakumar NR, Hee CW, Tan B, Liang WL, Gan GK. Direct fabrication of surface-relief grating by interferometric technique using femtosecond laser. Applied Physics A 2003;77:959–63.
[12] Wang XH, Chen F, Liu HW, Liang WW, Yang Q, Si JH, et al. Fabrication of micro-gratings on Au–Cr thin film by femtosecond laser interference with different pulse durations. Applied Surface Science 2009;255:8483–7.
[13] Her TH, Finlay RJ, Wu C, Deliwala S, Mazur E. Microstructuring of silicon with femtosecond laser pulses. Applied Physics Letters 1998;73:1673–5.
[14] Lee S, Yang D, Nikumb S. Femtosecond laser micromilling of Si wafers. Applied Surface Science 2008;254:2996–3005.
[15] Costache F, Kouteva-Arguirova S, Reif J. Sub-damage-threshold femtosecond laser ablation from crystalline Si: surface nanostructures and phase transformation. Applied Physics A: Materials Science and Processing 2004;79:1429–32.
[16] Crawford THR, Haugen HK. Sub-wavelength surface structures on silicon irradiated by femtosecond laser pulses at 1300 and 2100 nm wavelengths. Applied Surface Science 2007;253:4970–7.
[17] Baldacchini T, Carey JE, Zhou M, Mazur E. Superhydrophobic surfaces prepared by microstructuring of silicon using a femtosecond laser. Langmuir 2006;22:4917–9.
[18] Nunes B, Serro AP, Oliveira V, Montemor MF, Alves E, Saramago B, et al. Ageing effects on the wettability behavior of laser textured silicon. Applied Surface Science 2001;257:2604–9.
[19] Wu C, Crouch CH, Zhao L, Mazur E. Visible luminescence from silicon surfaces microstructured in air. Applied Physics Letters 2002;81:1999–2001.
[20] Zorba V, Alexandrou I, Zergioti I, Manousakia A, Ducatib C, Neumeister A, et al. Laser microstructuring of Si surfaces for low-threshold field-electron emission. Thin Solid Films 2004;453–454:492–5.
[21] Tan B, Sivakumar NR, Venkatakrishnan K. Direct grating writing using femtosecond laser interference fringes formed at the focal point. Journal of Optics A: Pure and Applied Optics 2005;7:169–74.
[22] Lee GJ, Park J, Kim EK, Lee Y, Kim KM, Cheong H, et al. Microstructure of femtosecond laser-induced grating in amorphous silicon. Optics Express 2005;13:6445–53.
[23] Choi YK, Zhu J, Grunes J, Bokor J, Somorjai GA. Journal of Physical Chemistry 2003;107:3340–3.
[24] Polushkin NI, Oliveira V, Conde O, Vilar R, Drozdov YN, Apolinário A, et al. Evidences for direct magnetic patterning via diffusive transformations using femtosecond laser interferometry. Applied Physics Letters 2012;101:132408.
[25] Sanchez F, Morenza JL, Aguiar R, Delgado JC, Varela M. Dynamics of the hydrodynamical growth of columns on silicon exposed to ArF excimer-laser irradiation. Applied Physics A: Materials Science and Processing 1998;66:83–6.
[26] Wysocki G, Denk R, Piglmayer K, Arnold N, Bauerle D. Single-step fabrication of silicon-cone arrays. Applied Physics Letters 2003;82:692–3.
[27] Kiani A, Venkatakrishnan K, Tan B. Direct patterning of silicon oxide on Si-substrate induced by femtosecond laser. Optics Express 2010;18:1872–8.
[28] Kiani A, Venkatakrishnan K, Tan B, Venkataramanan V. Maskless lithography using silicon oxide etch-stop layer induced by megahertz repetition femtosecond laser pulses. Optics Express 2011;19:10834–42.